A New Proposal to Jefferson Lab PAC-25

Measurement of G_E^p/G_M^p using elastic $\vec{p}(\vec{e}, e'p)$ up to $Q^2 = 3.2$ (GeV/c)^2

$\star\star\star$ **DRAFT** October 31, 2003$\star\star\star$

X. Zheng[1]
Argonne National Laboratory, Argonne, IL 60439

John Calarco
University of New Hampshire, Durham, NH 03824

Abstract

We propose here measurements G_E^p/G_M^p via doubly polarized elastic $\vec{p}(\vec{e}, e'p)$ scattering at $Q^2 = 2.1$ and 3.2 (GeV/c)^2. The UVa polarized NH_3 target will be used in Hall C with its spin aligned 42° w.r.t. beam direction. To extract G_E^p/G_M^p, we perform coincidence measurements at kinematics where the elastic asymmetries are the most sensitive to this ratio and the beam time needed is minimized. In addition, the asymmetry will be measured at $Q^2 = 0.72$ (GeV/c)^2 to determine the absolute electron beam helicity state and to check the product of beam and target asymmetries. Assuming 80% beam polarization and 85 nA current, we request 25 days of total beam time to achieve precision of $\Delta(G_E^p/G_M^p) = 0.05$ and 0.07 at $Q^2 = 2.1$ and 3.2 (GeV/c)^2, respectively. We request five days overhead time. The proposed measurement will provide the first data of G_E^p/G_M^p from the $\vec{p}(\vec{e}, e'p)$ asymmetry method in intermediate Q^2 range to a good precision. The new method is possiblly less sensitive to the two-photon exchange effect than Rosenbluth separation and it has different systematic uncertainties than polarization transfer method, hence will complement these two technique and provide valuable information on the proton form factors.

Contents

[1]Email: xiaochao@jlab.org

1 Motivation

The elastic form factors of the nucleon play an important role not only in hadronic physics as key input to our understanding of the nucleon structure, but also serve to test the Standard Model. However, there appear to be a discrepancy between previous data that clearly indicate a problem in either experimental methods or theories that were used to extract form factors from data. In this section we briefly review available calculations for G_E^p/G_M^p, then give an overview of previous world data and propose a new method to measure G_E^p/G_M^p.

1.1 Theories

The proton elastic form factors have been calculated in various models. At $Q^2 < 1$ (GeV/c)^2, the Vector Meson Dominance (VMD) model [1] successfully describes the nucleon form factors. In the high Q^2 region, the dominant degrees of freedom of the nucleon are the three valence quarks and perturbative Quantum Chromo-Dynamics (pQCD) theory can be applied [2]. Specifically, based on the leading-order pQCD, or hadron helicity conservation, the ratio of Dirac and Pauli

form factors F_2^p/F_1^p is expected to scale as $1/Q^2$ at high Q^2 [2, 3], which directly constrain the behavior of G_E^p/G_M^p.

In the intermediate region $1 < Q^2 < 20$ (GeV/c)^2, however, predictions for nucleon form factors become difficult because the soft scattering processes are still dominant compared to hard scattering. Moreover, this soft contributions might be different for different observables of the scattering processes. This fact itself can be used as a tool to understand the role of the soft parts of the nucleon without reaching asymptotically high Q^2. Many QCD models have been used to calculate the elastic nucleon form factors - the relativistic constituent quark model (RCQM) [4, 5], the cloudy bag model (CBM) [8], the SU(6) breaking CQM [7], the point-form spectator approximation (PFSA) model based on the Goldstone boson exchange CQM [6], and the chiral soliton model [9]. Currently, an axial-VMD model is being developed to estimate the effect of the two-photon exchange [10]. Figure 1 shows existing calculations for G_E^p/G_M^p along with world data.

Figure 1: Previous world data for G_E^p/G_M^p compared with various calculations including that from VMD (black) [1], the cloudy bag model [8], RCQM (red curve) [5], PSFA (green) [6], SU(6) breaking with CQM fFF (blue) [7] and chiral soliton model (magenta) [9]. Data below $Q^2 = 1$ (GeV/c)^2 are not shown for clarity.

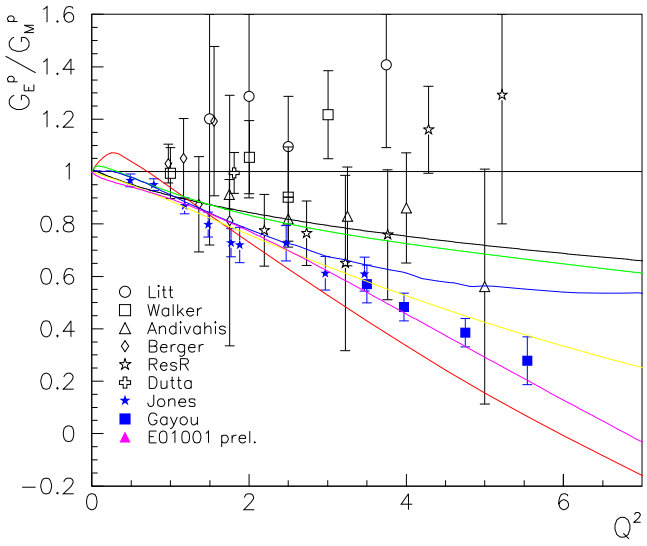

1.2 Existing Data

The proton elastic form factors have been measured for almost four decades. In the traditional Rosenbluth separation method, the elastic cross section is measured at fixed four momentum transfer Q^2 but different values of photon polarization ϵ, then the values of G_E^p, G_M^p and their

ratio are extracted from a linear fit of the cross section as a function of $1/\epsilon$. This method is usually used at $Q^2 < 9$ (GeV/c)^2. Data from this method show that G_M^p can be approximated by a dipole form $G_D = \mu_P/(1 + Q^2/0.71)^2$ with μ_P the proton magnetic moment and the ratio $\mu^p G_E^p/G_M^p$ is close to unity. Above this Q^2 region, G_M^p is extracted from single cross section measurements assuming $\mu^p G_E^p = G_M^p$. Data F_1^p at $Q^2 > 10$ (GeV/c)^2 show a $1/Q^4$ scaling behavior which is consistent with pQCD predictions [11].

However, recent data from polarization transfer method [12, 13, 14] showed that G_E^p/G_M^p drops linearly as Q^2 increases and reaches as low as ≈ 0.3 at $Q^2 = 5.6$ (GeV/c)^2, in significant disagreement with the Rosenbluth data (see Fig. 2). This dramatic change has invoked large interest in the proton form factor in both theoretical and experimental aspects. Different fits have been performed separately to data from Rosenbluth method, and data from both Rosenbluth and polarization transfer methods [17]. Previous Rosenbluth data have been re-analyzed [15] but the results are still inconsistent with polarization measurements. At high Q^2, data from cross section measurements have also been re-analyzed using the polarization transfer fit [13] and are found to be self-consistent [15]. The validity of radiative corrections has been checked and it has been suggested that the two-photon exchange process may explain part of the discrepancy between the two data sets. Experimentally, preliminary results from the recently accomplished Hall A experiment E01-001 [18] [2] agree well the traditional Rosenbluth data. More polarization transfer experiment [19] is being planned in Hall C to measure G_E^p/G_M^p via polarization transfer up to $Q^2 = 9.0$ (GeV/c)^2, using instrumentation independent from the Hall A experiments.

1.3 Two-Photon Exchange Correction

In order to explain the discrepancy between the Rosenbluth and the polarization transfer (p.t.) data, significantly effort has been put on understanding the radiative corrections and soft processes that can dilute the one-photon exchange process. Currently understanding is that there is at least a two-photon exchange process that was not accounted for in the Rosenbluth separation. This correction can introduce an ϵ-dependence to the cross sections and affect the linearity of Rosenbluth plot. Guichon and Vanderhaeghen [20] showed that, phenomenologically, the correction to Rosenbluth data is much larger than to p.t. data, and the true G_E^p/G_M^p is about 20% below the p.t. fit. Blunden, Melnitchouk and Tjon [21] evaluated the two-photon exchange contributions to elastic $e-p$ scattering cross sections based on a simple hadronic model including the finite size of the proton. Their results explained one third of the descrepancy between the two data sets. Rekalo and Tomasi-Gustaffson [22] derived from first principles, as the C-invariance of the EM interaction and the crossing symmetry, the general properties of two-photon exchange in $e-p$ elastic scattering. They showed again that the presence of this mechanism destroys the linearity of the Rosenbluth separation but does not aftfect the terms related to the EM form factors.

The two-photon exchange correction not only affect the extraction of form factors from $e-p$ scattering, but also affect many other observables, *e.g.* parity-violating asymmetries. A full

[2] sorry, data not available for plots in draft version

Figure 2: Previous world data for G_E^p/G_M^p from Rosenbluth method (open b&w markers) and from polarization transfer (solid b&w markers). For clarity, data below $Q^2 = 1$ (GeV/c)^2 are not shown. Preliminary results from recent Hall A E01-001 (solid magenta triangles) agree well with Rosenbluth data. Curves are from Bosted parameterization (black) [16], a fit to the Hall A polarization transfer results (blue) [13] and global fits to only Rosenbluth data (red) and both data sets (magenta) [17]. A dramatic disagreement is clearly seen between the two data set at $Q^2 > 2$ (GeV/c)^2.

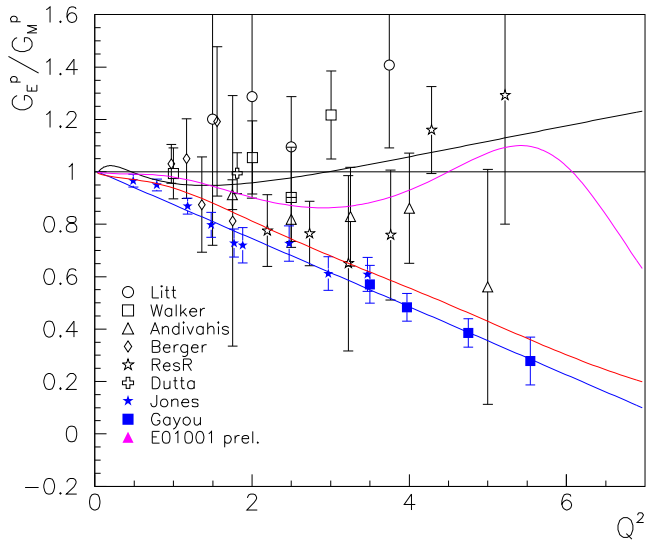

understanding of this process may take decades. Along this journey, experimental data will provide valuable and necessary guidance to the development of related theories. Moreover, there might be other corrections which we are not aware of, that can cause the desprepancy between the two form factor data sets. Therefore we think it is necessary to perform another measurement using a method different from Rosenbluth and polarization transfer.

1.4 The Proposed Experiment

We propose here a third method to measure G_E^p/G_M^p in the intermediate Q^2 range at $Q^2 = 2.1$ and 3.2 (GeV/c)^2. We will perform coincidence measurements and the G_E^p/G_M^p ratio will be extracted from measured elastic $\vec{e} - \vec{p}$ asymmetries. The UVa polarized NH_3 target will be used with its spin aligned at 42° w.r.t. beam-line (*i.e.* pointing downstream and to the left of the beam-line when viewing toward beam dump). In addition, the asymmetry at $Q^2 = 0.72$ (GeV/c)^2 will be measured inclusively to better than 2% statistical level, which serve to determine the absolute electron helicity state and to check the product of beam and target polarizations.

Assuming 85 nA beam current with 80% polarization, we request 25 days beam time to reach

$\Delta(G_E^p/G_M^p) = 0.05$ and 0.07 at $Q^2 = 2.1$ and 3.2 (GeV/c)^2, respectively. The above beam time include nitrogen runs and Møller measurements. Five days overhead time are needed for beam pass change and target work. The UVa polarized NH_3 target will be installed with un-parallel spin orientation.

The proposed measurement will provide the first data on G_E^p/G_M^p from a third method in the intermediate Q^2 range to a good precision. This method is possiblly less sensitive to the two-photon exchange effect than Rosenbluth separation, also it has different systematic uncertainties compared to polarization transfer technique, hence will complement these two methods. The new results will provide crucial information on both the proton structure and the understanding of previous world data. They will also provide valuable guidance for theoretical work on this topic.

2 Doubly polarized elastic scattering

For elastic scattering the unpolarized cross section is given by

$$\Big(\frac{\mathrm{d}\sigma}{\mathrm{d}\Omega \mathrm{d}E'}\Big)^u = \sigma_M \frac{E'}{E}\Big(\frac{G_E^2 + \tau G_M^2}{1+\tau} + 2\tau G_M^2 \tan^2(\theta/2)\Big)\,, \tag{1}$$

where $Q^2 = 4EE'\sin^2(\theta/2)$, $\tau = Q^2/(4M^2)$, the energy of scattered electrons is $E' = E/[1 + \frac{2E}{M}\sin^2(\theta/2)]$, M is the nucleon mass, E is the beam energy and θ is the electron scattering angle. The Mott cross section is

$$\sigma_M \equiv \Big(\frac{\mathrm{d}^2\sigma}{\mathrm{d}\Omega}\Big)_{Mott} = \frac{\alpha^2 \cos^2\frac{\theta}{2}}{4E^2 \sin^4\frac{\theta}{2}}\,. \tag{2}$$

The momentum and the angle of the scattered protons are

$$p_p = \sqrt{Q^2 + (\frac{Q^2}{2M})^2}\ \text{and} \tag{3}$$

$$\cos\theta_p = \frac{(M+E)\sqrt{M^2+p_p^2} - M^2 - ME}{p_p E}\,. \tag{4}$$

For the case of polarized electrons scattering off a polarized nucleon target, the cross section difference between opposite electron helicity states is given by

$$\sigma^+ - \sigma^- = -2\sigma_M \frac{E'}{E}\sqrt{\frac{\tau}{1+\tau}}\tan\frac{\theta}{2}\Bigg\{\sqrt{\tau(1+(1+\tau)\tan^2\frac{\theta}{2})}\cos\theta^\star G_M^2 + \sin\theta^\star\cos\phi^\star G_M G_E\Bigg\}\,, \tag{5}$$

and the asymmetry is

$$A \equiv \frac{\sigma^+ - \sigma^-}{\sigma^+ + \sigma^-} = -\frac{\sqrt{\frac{\tau}{1+\tau}}\tan\frac{\theta}{2}\left\{\sqrt{\tau(1+(1+\tau)\tan^2\frac{\theta}{2})}\cos\theta^\star G_M^2 + \sin\theta^\star\cos\phi^\star G_M G_E\right\}}{\frac{G_E^2+\tau G_M^2}{1+\tau} + 2\tau G_M^2\tan^2(\theta/2)}\,, \quad (6)$$

where the superscript $\pm$ denotes the helicity of the incident electrons, θ^* and ϕ^* are the polar and the azimuthal angles of the target spin direction as shown in Fig. 3. The scattering plane is

Figure 3: Polar and azimuthal angles of the target spin. Here $\vec{S}$ is the target spin, $\vec{q}$ is the three momentum transfer. The $z\star$ axis is defined by $\vec{q}$, $y\star$ axis is defined by $\vec{k}\times\vec{k}'$ with $k(k')$ the three momentum of the incident and scattered electrons.

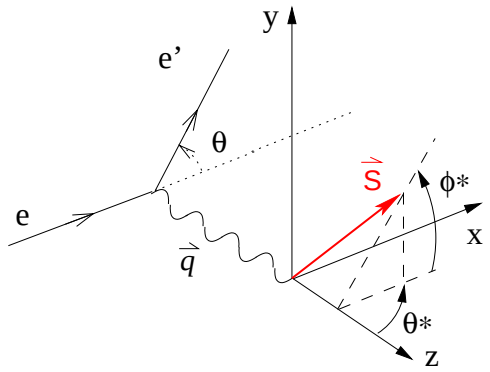

defined by the q-vectors of electrons. Equation (6) can be written as

$$(\frac{G_E}{G_M})^2 + B(\frac{G_E}{G_M}) + C = 0\,, \quad (7)$$

where

$$B = \frac{1}{A}\sqrt{\tau(1+\tau)}\tan\frac{\theta}{2}\sin\theta^\star\cos\phi^\star\,, \quad (8)$$

$$C = \tau + 2\tau(1+\tau)\tan^2\frac{\theta}{2} + \frac{\cos\theta^\star}{A}\left\{\sqrt{\tau(1+\tau)}\tan\frac{\theta}{2}\sqrt{\tau\left[1+(1+\tau)\tan^2\frac{\theta}{2}\right]}\right\} \quad (9)$$

with A the measured elastic asymmetry. Therefore ratio G_E/G_M can be calculated as

$$\frac{G_E}{G_M} = \frac{1}{2}(-B \pm \sqrt{B^2-4C})\,, \quad (10)$$

the sign is kinematic dependent. The uncertainty is given by

$$\Delta(\frac{G_E}{G_M}) = \frac{\Delta A}{2}\left|\left(\frac{\mathrm{d}B}{\mathrm{d}A}\right)\left(-1 \pm \frac{B}{\sqrt{B^2-4C}}\right) \pm \left(\frac{\mathrm{d}C}{\mathrm{d}A}\right)\frac{-2}{\sqrt{B^2-4C}}\right| \quad (11)$$

$$\text{where} \qquad \frac{\mathrm{d}B}{\mathrm{d}A} = -\frac{B}{A}$$

$$\text{and} \qquad \frac{\mathrm{d}C}{\mathrm{d}A} = -\frac{C - [\tau + 2\tau(1+\tau)\tan^2\frac{\theta}{2}]}{A}$$

3 Experimental Setup

In this section we describe the experimental setup for the proposed measurement in Hall C.

3.1 Overview

The floor plan for Hall C is shown in Fig. 5. The UVa polarized NH_3 target will be installed with its spin direction aligned at 42° w.r.t. beam-line. For coincidence measurement, the scattered electrons are detected by a calorimeter and the protons by HMS. Elastic events are identified by the proton momentum and the electron scattering angle.

Figure 4: Hall C floor plan for the proposed measurement (not to scale).

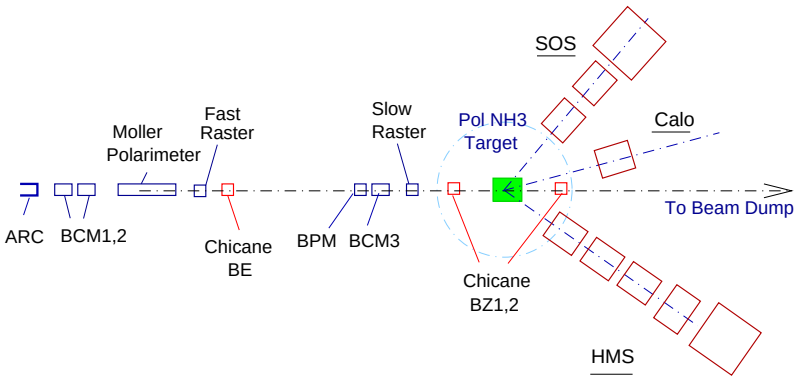

3.2 Beam Line

We propose to use polarized beam with 80% polarization and 85 nA beam current at three beam energies, 1.162, 5.562, and 5.562 GeV. Beam energy will be measured to $\Delta E/E = 2 \times 10^{-4}$ level using ARC method [23]. We plan to use Møller for beam polarization measurement. Currently the Møller polarimeter in Hall C can provide better than 1% precision. However additional systematic error can come from the fact that we are running at 85 nA low current. We therefore use 1.5% in the uncertainty estimation.

Because the target spin is not parallel to the beam direction, the strong 5 T magnetic field of the target will bend the electron beam toward the floor. In order to ensure that the incoming beam is incident on the target cell horizontally, we will use a chicane magnet to bend the beam

Figure 5: Kinematics of the proposed measurement. Target spin angles are shown for the case when scattering plane is horizontal. Lightly shaded area shows the blocking of target coils, which covers from 50° to 73° along either side of the field axis.

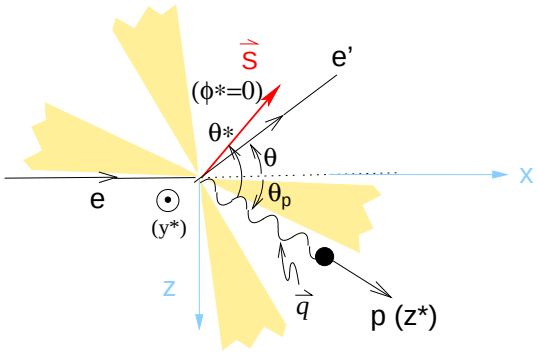

Figure 6: Hall C beam line chicane magnets and raster system.

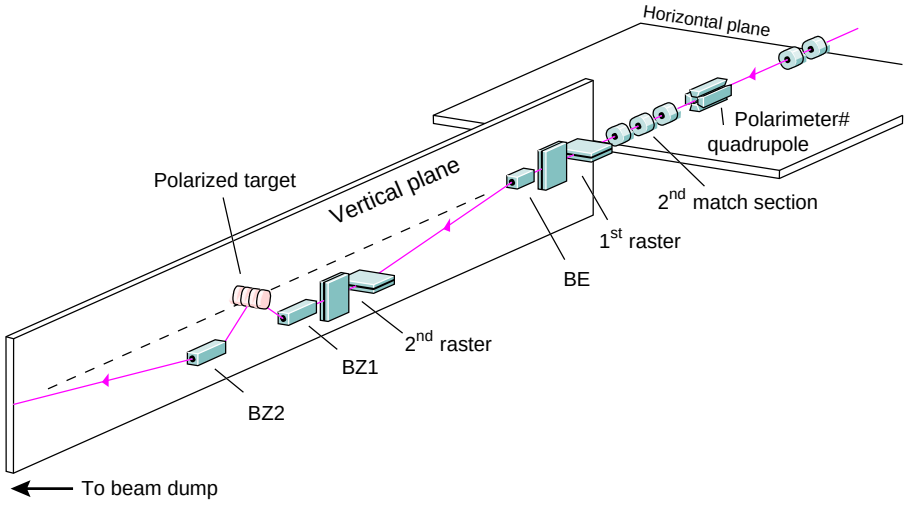

up before it enters the target scattering chamber. In addition, the beam will be bend again after it exits the target such that it will arrive in the beam dump. A series of chicane magnets were used for similar purpose during the G_E^n experiment E93-026 [25, 26] and we will use the same setup.

The beam needs to be rastered to maintain the target polarization and to ensure uniform distribution of both heat and radiation on the target material. We require the beam spot at the target to be $\approx$ 2 cm in diameter which is almost the entire target. This was achieved using the slow rastering system during previous experiments [25, 26]. A schematic diagram for the beam-line chicane magnets and raster system is shown in Fig. 6.

Beam position monitoring and beam current measurement at our low current of 85 nA need special care. Using the same method as previous experiment E93-026, we believe a precise beam position monitoring can be achieved and the beam current can be measured to 5% level. The effect on the measured asymmetry should be negligible.

3.3 The UVa NH_3 Target

We will use a solid polarized proton target developed by the University of Virginia. In this target, Dynamic Nuclear Polarization (DNP) is utilized to enhance the low temperature ($\approx$ 1 K), high magnetic field (5 T) polarization of solid materials. The irradiation of the target with 140 GHz microwaves drives hyperfine transitions hence align the nucleon spins. This target was successfully used in the SLAC experiments E143, E155 and E155x and two experiments E93-026 [25] and E01-006 [26] at Hall C. The proton polarization in $^{15}NH_3$ can reach as high as 95% and will decrease because of the beam depolarization effect. An average polarization of 75% was routinely achieved during previous experiments.

The target consists of a superconducting dipole magnet which operates at 5 Tesla, a ^{4}He evaporation refrigerator, a large pumping system, a high power microwave tube operating at frequencies around 140 GHz and a NMR system for measuring the target polarization. Figure 7 shows the target side view.

For the proposed measurement, the target material is $^{15}NH_3$ and the target spin needs to be aligned at 42° w.r.t. beamline. The target polarization needed is 75% (average) with 85 nA beam, measured by NMR to 2.5% level. The target cell is a 3 cm long cylinder with 1 inch diameter. Figure 8 shows the geometry of the cell and the NMR coil used to measure proton polarization.

The target cell is filled by frozen ammonia granules and is placed into a target holder and lowered into a cryostat of liquid ^{4}He. The nitrogen, helium and other target holder materials are in the acceptance of the spectrometers and will serve to dilute the measured asymmetry. Thickness and density of each material are given in Table 1. Dilution factor will be given in Section 4.4. Moreover, the unpaired proton in nitrogen can be polarized, hence a correction to the asymmetry must be made during analysis. The uncertainty due to nitrogen asymmetry will be given in Section 4.5.

The strong magnetic field at this configuration will have an effect on the scattering charged particles but this can be well simulated and corrected.

We need to know the field direction to at least 1° and 0.5° is desirable.

Figure 7: Sideview of the UVa polarized NH_3 target.

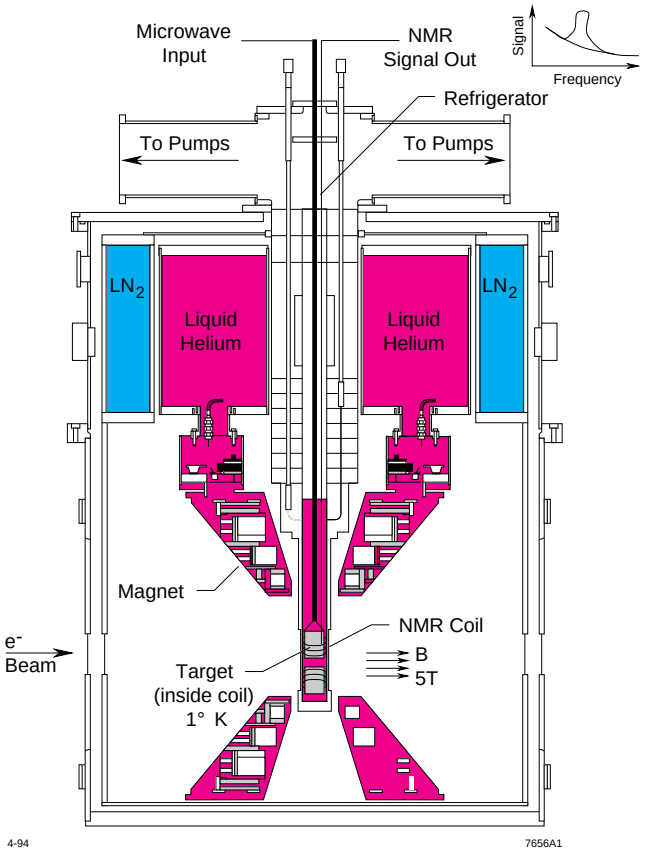

Figure 8: The 3 cm long by 1 inch diameter cylindrical target cell with the single loop coil used for measuring the proton polarization. Drawing not to scale.

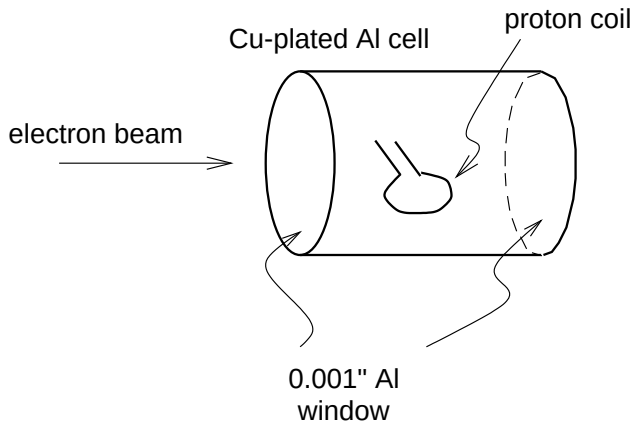

Table 1: Thickness and density for unpolarized materials in acceptance.

Material	Thickness (cm)	Density (g/cm^3)
^{4}He	0.37	0.145
Al end-caps	0.00762	2.70
Copper in NMR coil	0.00673	8.96
Nickel in NMR coil	0.00289	8.75
Titanium windows in tail	0.00712	4.54
Al windows in LN_2 shield	0.00508	2.70
Al entrance window in cryostat	0.00702	2.70
Al exit window in cryostat	0.01016	2.70

3.4 Spectrometer

For coincidence measurment, we plan to use a calorimeter to detect electrons and High Momentum Spectrometer (HMS) for protons. Elastic events are identified by the proton momentum. The electron scattering angle will help to reduce the quasi-elastic background. We need aerogel cherenkov detector in HMS (which is part of the standard equipment) for particle ID. The central momentum of the spectrometers can be calculated from the dipole field magnitude to 1×10^{-3} level [23]. The central angle can be determined to 0.3 mrad (?). For the proposed kinematics the angle and momentum resolutions are important since we rely on a cut in the elastic peak to minimize the dilution effect due to quasi-elastic events from other target material than protons. For the proposed two Q^2 points we have an angle sensitivity of $\mathrm{d}p_p/\mathrm{d}\theta_p \approx 5$ MeV/mrad hence the width of the elastic peak reconstructed from HMS has FWHM≈ 20 MeV for the elastic peak

which is sufficient for our measurement. In Section 4.4 we will estimate the dilution factor.

3.5 Electron Calorimeter

For the proposed measurement, electrons will be detected by a calorimeter. We plan to use part of the new calorimeter being built for the Hall-C high Q^2 G_E^p/G_M^p experiment [19]. Since for our kinemastics the electron phase space is smaller than that for the proton, the solid angle acceptance of the calorimeter does not need to be very large. However one need to take into account the bending of electrons due to target magnetic field.

The electron solid angle is related to that of the proton as

$$\frac{\mathrm{d}\Omega_p}{\mathrm{d}\Omega_e} = \frac{\mathrm{d}\theta_p}{\mathrm{d}\theta_e} = -2E'^{\,2}\sin(\theta_e)\Big(1+\frac{Q^2}{2M_p^2}\Big)\left[\frac{M_p(M_p+E)\Big(M_p+\sqrt{M_p^2+p_p^2}\Big)}{2Ep_p^3\sqrt{M_p^2+p_p^2}}\right] \quad (12)$$

Protons at $Q^2 = 2.1$ and 3.2 (GeV/c)^2 are bended up by 10.97° and 7.73°, respectively. So the elastically scattered electrons should have a positive (vertically up) out-of-plane angle. The target field will bend electrons down by 3.68 and 4.21. These two effects cancel so electrons should be detected in a vertical range from 0° to 10°. The horizontal angle will be $\pm 3^\circ$. The calorimeter is made of 3.9×3.9 cm^2 lead-glass blocks. We plan to place it at 10 m away from the target with $1/5$ below the level of target center. The angular resolution will be 4 mrad in both directions. We need 5(h)$\times$10(v) blocks for the proposed measurement.

3.6 Acceptance Effect due to Target Magnetic Field

Due to the strong magnetic field the scattered protons will be bended up by $\approx 5 \sim 7^\circ$, This will cause a tilt of the scattering plane. The direct effects are that there is a correction to the target spin polar angle $\theta^\star$ and $\phi^\star \neq 0$. Figure 9 shows HMS acceptance for protons at $Q^2 = 3.2$ (GeV/c)^2. The proton bending angle due to target field is small and the scattering angle is close to the HMS central setting.

3.7 Low Q^2 Measurement

We will measure elastic longitudinal asymmetry at $Q^2 = 0.72$ (GeV/c)^2 to 2% level to check the product of target and beam polarizations. The Short Orbit Spectrometer (SOS) will be used at single-arm mode to detect protons at 42°. Since protons are scattered parallel to the target spin direction, there is no bending effect from the magnetic field.

3.8 Data Analysis

The physics asymmetries can be extracted from the raw asymmetries as

$$A_{\parallel,\perp} = \frac{A_{raw}(1-\eta_{A_N})}{P_{beam}P_{targ}f} \quad (13)$$

Figure 9: HMS acceptance for $p = 2.471$ (GeV/c) protons with (red) and without (black) target field. With target field protons with initial $\phi_{targ} > 0$ (vertical down) will reach the center of HMS.

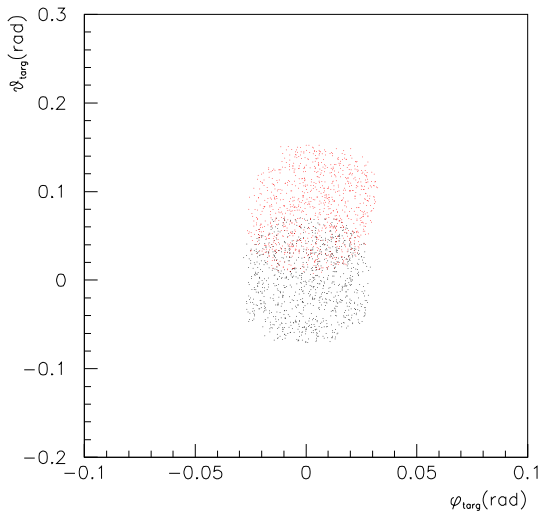

where $P_{beam} = 80\%$ and $P_{targ} = 75\%$ are beam and target polarization, f is the target dilution factor and η_{A_N} is a correction factor due to the asymmetry of nitrogen in $^{15}NH_3$ (see Section 4.5). Ratio G_E^p/G_M^p is extracted using Eq. (10) and its uncertainty from Eq. (11).

The error in asymmetry A is

$$\Delta A = \left\{ \left(\frac{\Delta A_{raw}}{f P_b P_t} \right)^2 + A^2 \left[(\frac{\Delta P_b}{P_b})^2 + (\frac{\Delta P_t}{P_t})^2 + (\frac{\Delta f}{f})^2 \right] \right\}^{1/2}, \quad (14)$$

$$\text{with} \qquad \Delta A_{raw} = \frac{1}{\sqrt{N}} \quad (15)$$

Here N is total number of events. The coincidence rate will be essentially determined by the HMS acceptance.

4 Expected Uncertainties and Rate Estimation

In this section we first estimate all systematic uncertainties. Then we calculate the rate, total uncertainties and beam time.

4.1 Experimental Systematics

We estimate the uncertainty in the beam polarization to be 1.5% and target polarization is 2.5%. Other error sources include those from the beam energy $\Delta E/E = 2 \times 10^{-4}$, the spectrometer central momentum $\Delta p_p/p_p = 1 \times 10^{-3}$ [23], and central angle $\Delta\theta = 0.3$ mrad. The target

spin angle can be measured to 0.5°. The uncertainty in Q^2 is given by Δp_p. The largest systematic uncertainty comes from target polarization. At $\Delta P_{targ}/P_{targ} = 2.5\%$ the uncertainty in G_E^p/G_M^p is about $2/3$ of the statistical uncertainty.

4.2 Beam Charge Measurement

The beam current can be measured to 5% level at 100 nA. The effect on the measured asymmetries is negligible.

4.3 Target Polarization

Target polarization can be measured to 2.5% using NMR.

4.4 Target Dilution Factor

The dilution factor is due to the quasi-elastic events from nitrogen in NH_3 and from other material listed in Table 1. Since the reconstructed elastic peak at forward angles typically has < 20 MeV FWHM, while quasi-elastic events are smeared by Fermi motion at $p_F/M = \pm 10\%$ level if Fermi momentum $p_F \approx 200$ MeV/c, about 90% of quasi-elastic events will be excluded using a cut in $\delta p \equiv p_p - p_{el}$ where p_p is the proton momentum measured by HMS and p_{el} is the momentum of elastically scattered proton calculated from the measured scattering angle θ_p. Moreover, since we are doing coincidence measurement, quasi-elastic events will be further suppressed by the electron phase space, which is constrained by the calorimeter. Figure 10 shows the simulated elastic events (red), quasi-elastic events (green) and the sum (blue) for 1 mC beam charge at $Q^2 = 3.2$ (GeV/c)^2.

The dilution factor is defined as

$$f = \frac{N_p}{N_p + N_{\rm QE}} \tag{16}$$

where N_p and $N_{\rm QE}$ are yield of $e-p$ elastic events and quasi-elastic from ^{15}N and other target material. In Table 2 we list the estimated dilution factor for different conditions. We use 0.93

Table 2: Dilution factor f at $Q^2 = 3.2$ (GeV/c)^2. Unit for δp is MeV/c and for $\delta\theta_e$ is rad. ******numbers are subject to change******

Q^2 (GeV/c)^2	2.1	3.2
single proton with $\delta p_p = (-50, -30)$	0.688	0.552
coin. with $\delta p_p = (-50, -30)$	0.895	0.754
coin. with $\delta p_p = (-50, -30)$ and $\delta\theta_e = (-0.03, 0.02)$	0.943	0.877

and 0.90 for $Q^2 = 2.1$ and 3.2 (GeV/c)^2 respectively in the rate and uncertainty estimation. For $Q^2 = 0.72$ single-arm measurement we use $f = 0.3$,

Figure 10: Expected spectra on $\delta p \equiv p_p - p_{p,el}$ for single-arm proton measurement (top) and coincidence measurement (middle), and on electron angle $\delta\theta_e = \theta_e - \theta_{e,el}$ for coincidence measurement after δp cut (bottom). Here p_p is measured proton momentum and $p_{p,el}$ is momentum for elastic scattering calculated from proton scattering angle. θ_e is measured electron scattering angle and $\theta_{e,el}$ is calculated electron angle from elastic conditions. Simulations were performed using SIMC without HMS collimators, ^{15}N and ^{4}He quasi-elastic events were simulated by ^{12}C spectral functions and all other material were using ^{56}Fe spectral function. The blue shows the sum of elastic and quasi-elastic events. The dilution f is given for: single-arm proton measurement with cut $\delta p = (-50, -30)$ MeV (top); coincidence measurement with cut $\delta p = (-50, -30)$ MeV (middle); and coincidence measurement with cut $\delta p = (-50, -30)$ MeV and $\delta\theta_e = (-0.03, 0.02)$ rad (bottom). Number of elastic counts in the bottom spectrum was used for rate estimation.

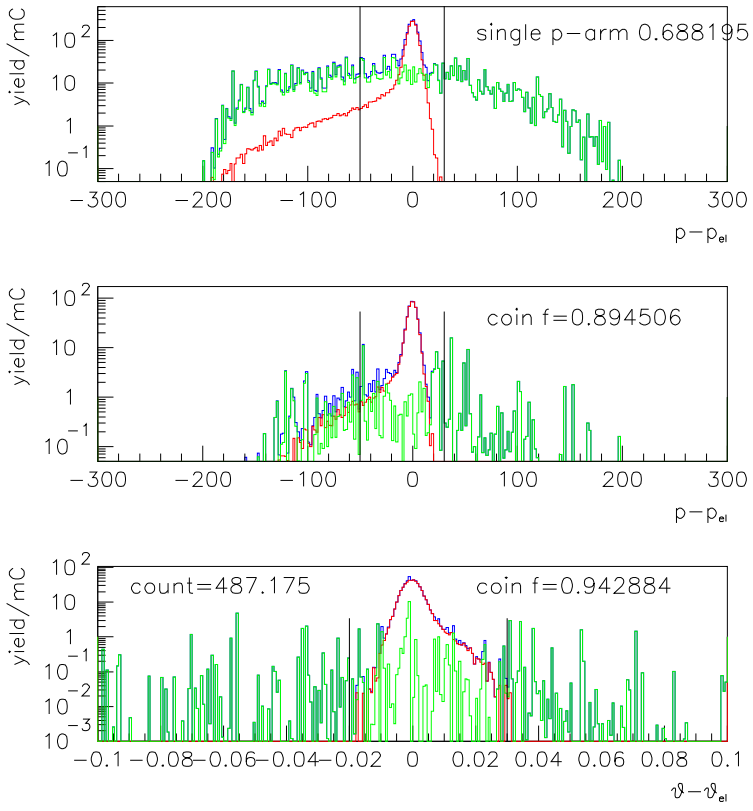

We will take data on a nitrogen cell with approximately the same geometry as NH_3 cell to measure quasi-elastic cross section from nitrogen and all other target material. If the measurement gives 4% uncertainty in the quasi-elastic yield, and from elastic events we measure elastic yield to 2% level, then the error on dilution factor is

$$\begin{aligned} \frac{\Delta f}{f} &= (1-f)\sqrt{(4\%)^2 + (2\%)^2} \\ &\approx (1-f) \times 4.4\% \, . \end{aligned} \tag{17}$$

giving $< 1\%$ for $Q^2 = 3.2$ (GeV/c)^2. For $Q^2 = 0.72$ the quasi-elastic yield will be large and we expect to achieve 2% uncertainty on N_{QE}, hence the error is $\Delta f/f \approx 2\%$.

4.5 Nitrogen Asymmetry

The nitrogen in NH_3 is polarized and will contribute to the asymmetry. In the shell model, ^{15}N nuclei has one unpaired proton which can be polarized. The polarization of the unpaired proton in ^{15}N is reduced from that of a free proton by several factors. First, the nitrogen in ^{15}N is polarized up to only $1/6$ of the proton, based on the Equal Spin Temperature (EST) hypothesis. Experimental data show even lower polarization, as shown in Fig. 11. Secondly, the proton

Figure 11: Polarization of nitrogen P_N in $^{15}NH_3$ *vs.* proton polarization P_p measured during E155 [28]. The black circle is the prediction in Equal Spin Temperature (EST) hypothesis and the red dots is what were actually measured.

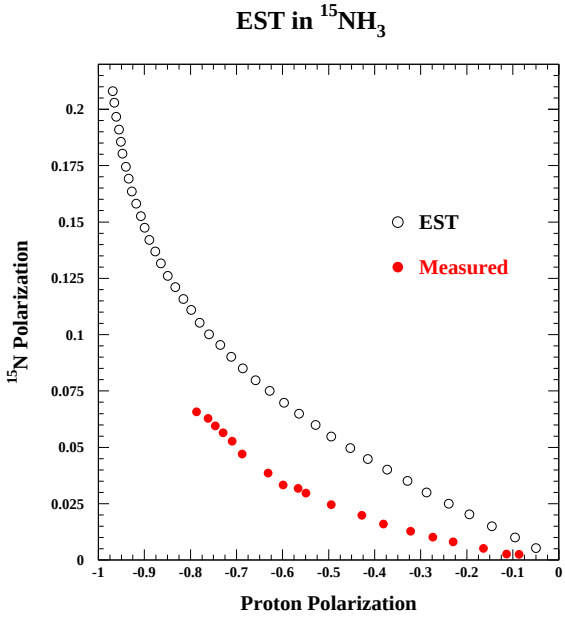

in a polarized ^{15}N is only polarized to a certain amount. This quantity, called the effective nucleon polarization, has been estimated in two ways. In a model independent method [29, 30], $P_{p/^{15}\mathrm{N}} \approx -0.22$ based on isospin symmetry and data from beta decay of the mirror nuclei ^{15}O. In the shell model, the proton in ^{15}N is aligned anti-parallel to the nuclear spin $1/3$ of the time, hence $P_{p/^{15}\mathrm{N}} = -0.33$. Overall, the polarization of the unpaired proton is at most $(0.22 \sim 0.33) \times 1/6 P_p = 0.037 \sim 0.055 P_p$ and if we take the measured data, is about $(0.22 \sim 0.33) \times 1/10 P_p = (0.022 \sim 0.033) P_p$. In addition, only about $1/7$ of ^{15}N quasi-elastic events are from the $p_{1/2}$ proton and ^{15}N contribute $\approx 60\%$ of all quasi-elastic events. Hence the correction to the measured asymmetry A_m due to nitrogen is

$$A_m = f A_p + \frac{0.6(1-f)}{7} A_{p/^{15}\mathrm{N}} = f A_p \Big(1 + (0.018 \sim 0.028)\frac{1-f}{f}\Big) \quad (18)$$

$$A_p = \frac{A_m}{f}\Big(1 - (0.0026 \pm 0.0006)\Big) \quad \text{if } f = 0.9 \quad (19)$$

Compared to the usually used $A = \frac{A_m}{f}$, we need to apply 0.26% correction with $\pm 0.06\%$ uncertainty for $Q^2 = 2.1$ and 3.2 (GeV/c)^2 points. For $Q^2 = 0.72$ (GeV/c)^2 the correction is $(5.4 \pm 1.2)\%$.

4.6 Background

For coincidence measurement, the main background comes from the quasi-elastic scattering from nitrogen and materials on the beam path. This part is stated in the last section. For single-arm proton measurement, we also have background from π^0 photoproduction. We estimate this background to be less than 1% based on data from the Hall A experiment E01-001. The π^+ background is expected to be small and will be rejected by Aerogel cherenkov detector so the effect on the measured asymmetry is negligible.

4.7 Electromagnetic Radiative Corrections

The EM radiative corrections were simulated using Mo&Tsai. The uncertainty in the radiative corrections on the asymmetries is negligible.

4.8 Deadtime Correction

The rate of our proposed measurement is very low, $\sim$Hz, hence the electronic dead time correction is small and the effect on the measured asymmetry is negligible. Computer deadtime can be measured by triggers and the uncertainty is determined by the statistics of each run. We require a run to have at least 1M events hence the uncertainty in the measured deadtime is 0.1%.

4.9 Kinematics, Rate Estimation and Expected Uncertainties

We use Bosted fit for G_M^p and the G_E^p/G_M^p value from polarization transfer data [13] to calculate the elastic $e-p$ cross section. Using 3 cm target cell and 85 nA the luminosity available is

Table 3: Kinematics, rate and expected uncertainties for the proposed measurements.

Q^2 (GeV/c)^2	0.72	2.1	3.2
E_b (GeV)	1.162	5.562	5.562
$\theta_{e,inp}$	-	12.76°	20.95°
$(\theta_{e,tot})$	-	(16.76°)	(22.27°)
$(\theta_{e,oop})$	-	(10.97°)	(7.73°)
E' (GeV)	-	4.443	3.857
$\theta_{p,inp}$	42.00°	43.31°	35.53°
$(\theta_{p,tot})$	(42.00°)	(44.41°)	(36.26°)
$(\theta_{p,oop})$	(0)	(-10.97°)	(-7.73°)
p_p (GeV/c)	0.929	1.831	2.471
$\theta^\star$	0°	85.89°	78.00°
$\phi^\star$	0°	-7.31°	-5.16°
A_{el}	-0.283	-0.064	-0.098
$(A_{el,bosted})$	-0.283	-0.075	-0.123
A_{raw}	-0.051	-0.0359	-0.0529
σ (nb/sr)	9.440	4.820	0.453
coin rate (Hz) (SIMC)	7.4	1.4182	0.1837
N_{coin}	964K	589K	269K
Uncertainty on asymmetries Statistical	2.0	3.634%	3.643%
Uncertainty on G_E^p/G_M^p			
$\Delta P_{beam}/P_{beam} = 1.5\%$	-	0.0175	0.0211
$\Delta P_{targ}/P_{targ} = 2.5\%$	-	0.0292	0.0352
Target dilution $\Delta f/f = 1\%$	-	0.0117	0.0141
Nitrogen asymmetry	-	0.0007	0.0008
Deadtime correction	-	0.0012	0.0014
$\Delta p_p/p_p = 1 \times 10^{-3}$	-	0.0018	0.0005
$\Delta\theta_e = 1$ mrad	-	0.0018	0.0013
Target spin orientation (inp) 0.5°	-	0.0123	0.0131
Target spin orientation (oop) 0.1°	-	0.0011	0.0006
Total stat.	-	0.0425	0.0513
Beam time (days)	1.5	4.8	17.0
Expected G_E^p/G_M^p and total uncertainty	-	0.732 ± 0.054	0.589 ± 0.065

$\diamond$ E_b is beam energy;
$\diamond$ θ_e and E' are the energy and momentum of scattered electrons (SOS);
$\diamond$ θ_p and p_p are the energy and momentum of scattered protons (HMS);
$\diamond$ $\theta^\star$ and $\phi^\star$ are the polar and azimuthal angles of target spin;
$\diamond$ A_{el} and $A_{el,bosted}$ are elastic asymmetries calculated from Hall A polarization transfer fit and bosted fit, respectively;
$\diamond$ A_{raw} is expected measured asymmetry using PT fit;
$\diamond$ N is total number of coincidence events;

8.5×10^{34} cm^2/s. Kinematics, rates and expected uncertainties for the proposed measurements are given in Table 3. The expected results are shown in Fig. 12.

Figure 12: Expected results and full uncertainties of the proposed measurements, compared with all data. Red points are results if measured asymmetries agree with polarization transfer and green ones are for the case if measured asymmetries are half way in between. Curves are the same as in Fig. 2.

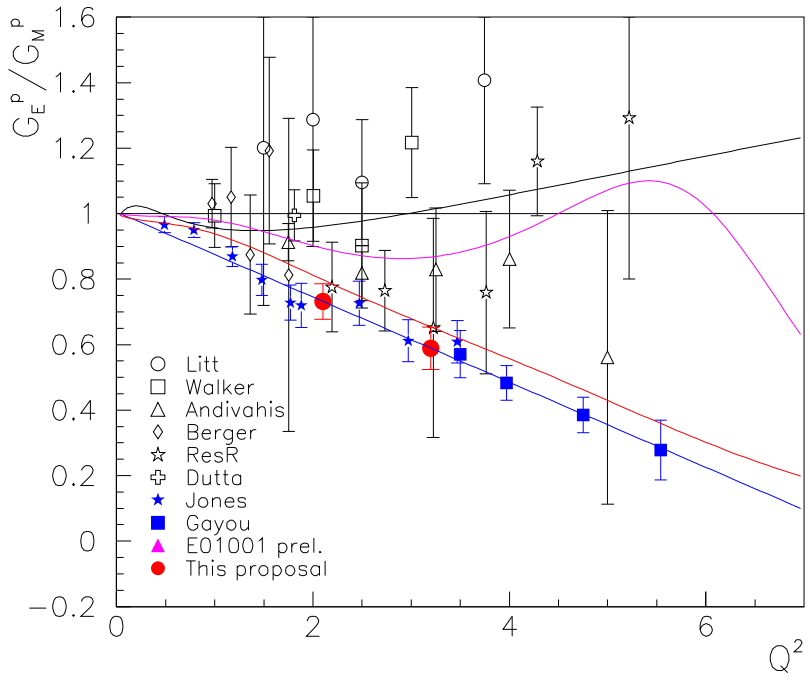

5 Comparison to other Methods

In the following we compare the proposed measurement with other possible methods using doubly polarized scattering.

In principle, G_E/G_M is directly related to the ratio of transverse ($\theta^\star = 90$) and longitudinal ($\theta^\star = 0$) asymmetries A_T/A_L, as can be seen from in Eq. (10) and (11). However to achieve the same uncertainty in G_E^p/G_M^p, one needs to measure ratio A_L/A_T to the same relative level as the asymmetry A_{pr} in our proposed measurement. In this case, the absolute error in A_T is magnified by factor $1/A_L$ therefore will need more beam time.

In addition, using coincidence method that we proposed here, the background events will be largely suppressed and the dilution effect caused by the unpolarized material (all have $A > 1$) is much smaller than single arm measurement. For example, at $Q^2 = 3.2$ (GeV/c)^2 dilution factor is $f \approx 0.5$ for single arm proton measurement[3], $f \approx 0.3$ for single arm electron measurement (the quasi-elastic counts are doubled compare to single proton case since the neutrons in ^{15}N also contribute), and $f > 0.9$ for coincidence case. Overall, the proposed measurements will give the best results with the least resources.

6 Beam Time Request

Our beam time request is given in Table 4. We ask for 25 days total beam time, including production data taking, target dilution factor measurement and Møller measurement. We ask for 5 days overhead time for beam energy change and measurement of the target field direction. Time needed for target installation is not given here.

7 Summary

We propose here measurements G_E^p/G_M^p via doubly polarized elastic $\vec{p}(\vec{e}, e'p)$ scattering at $Q^2 = 2.1$ and 3.2 (GeV/c)^2. Assuming 80% beam polarization and 85 nA current, we request 25 days of total beam time and five days overhead. The proposed measurement will provide the first data of G_E^p/G_M^p from the $\vec{p}(\vec{e}, e'p)$ asymmetry method in intermediate Q^2 range to a good precision. The new method is less sensitive to the possible two-photon exchange effect than Rosenbluth separation and it does not suffer from systematic uncertainties due to spin pro-

[3]note that one also have π^0 production background which has < 10 MeV threshold and cannot be excluded cleanly using δp cut, while keep certain statistics. We did not simulate this background because it will be eliminated to negligible level for coincidence case.

Table 4: Beam time request (in hours) for the proposed measurements.

Q^2 (GeV/c)^2	0.72	2.1	3.2
Production time	36.1	115.3	407.1
nitrogen run	6	6	6
Møller measurement	6	6	6
arc measurement	4	4	4
Total beam time		600	
Energy change		36	
Target anneal		54	
Target field direction		12	
Spectrometer angle survey		?	
Total overhead		102	

cession which exist in previous polarization transfer data.

Acknowledgment

References

[1] E.L. Lomon, *Phys. Rev. C* **64**, 035204 (2001).

[2] S.J. Brodsky and G. Farrar, *Phys. Rev. D* **11**, 1309 (1975).

[3] S.J. Brodsky and G.P. Lepage, *Phys. Rev. D* **22**, 2157 (1981).

[4] P.L. Chung and F. Coester, *Phys. Rev. D* **44**, 229 (1991).

[5] M.R. Frank, B.K. Jennings and G.A. Miller, *Phys. Rev. C* **54**, 920 (1996).

[6] R.F. Wagenbrunn *et al.*, *Phys. Lett. B* **511**, 33 (2001); S. Boffi *et al. Eur. Phys. J. A* **14**, 17 (2002), or e-Print hep-ph/0108271

[7] F. Cardarelli and S. Simula, *Phys. Rev. C* **62**, 065201 (2000); S. Simula, e-Print nucl-th/0105024.

[8] D.H. Lu, A.W. Thomas and A.G. Williams, *Phys. Rev. C* **57**, 2628 (1998).

[9] G.Holzwarth, *Zeitschr. Fuer Physik A* **356**, 339 (1996), e-Print hep-ph/9606336; e-Print hep-ph/0201138 and ref. therein.

[10] A. Afanasev, *priv. comm.*

[11] A.F. Sill *et al.*, *Phys. Rev. D* **48**, 29 (1993).

[12] M. K. Jones *et al.*, *Phys. Rev. Lett.* **84**, 1398 (2000), e-Print: nucl-ex/9910005;

[13] O. Gayou *et al.*, *Phys. Rev. Lett.*, **88**, 092301 (2002), e-Print: nucl-ex/0111010.

[14] O. Gayou *et al.*, *Phys. Rev. C* **64**, 038202 (2003).

[15] J. Arrington, *Eur. Phys. J.* **A17**, 311 (2003), e-Print Archive: hep-ph/0209243; *Phys. Rev.C* **68**, 034325 (2003), e-Print Archive: nucl-ex/0305009;

[16] P. Bosted, *Phys. Rev. C* **51**, 409 (1995).

[17] H. Budd, A. Bodek and J. Arrington, *to be published in Nucl. Phys. B*, e-Print Archive: hep-ex/0308005.

[18] J. Arrington and R. Segel, JLab E01-001, New Measurement of (GE/GM) for the Proton.

[19] E. Brash, C. Perdrisat and V. Punjabi, JLab E01-109, Measurement of Gep/Gmp to Q2=9 GeV2 via Recoil Polarization.

[20] P.A.M. Guichon and M. Vanderhaeghen, e-Print: hep-ph/0306007.

[21] P.G. Blunden, W. Melnitchouk and J.A. Tjon, e-Print:nucl-th/0306076.

[22] M.P. Rekalo and E. Tomasi-Gustafsson, e-Print:nucl-th/0307066.

[23] Here should go a Hall C NIM paper;

[24] H.-G. Zhu, *Ph.D. thesis*, Univ. of Virginia, Charlottesville, VA (2000).

[25] D. Day, JLab E93-026, The Charge Form Factor of the Neutron.

[26] O. Rondon-Aramayo, JLab E01-006, Precision Measurement of the Nucleon Spin Structure Functions in the Region of the Nucleon Resonances.

[27] P.E. Raines, *Ph.D. thesis*, Univ. of Pennsylvania, (1996).

[28] H.-G. Zhu, *priv. comm.*

[29] K. Sugimoto, *Phys. Rev.* **182**, 1051 (1969).

[30] O.A. Rondon, *Corrections to nucleon spin structure asymmetries measured on nuclear polarized targets*, unpublished.